UNDERSEA ROBOTICS

Rotary-actuated folding polyhedrons for midwater investigation of delicate marine organisms

Zhi Ern Teoh[1,2]*, Brennan T. Phillips[3], Kaitlyn P. Becker[1,2], Griffin Whittredge[1,2], James C. Weaver[1,2], Chuck Hoberman[2,4], David F. Gruber[5,6], Robert J. Wood[1,2]

Self-folding polyhedra have emerged as a viable design strategy for a wide range of applications, with advances largely made through modeling and experimentation at the micro- and millimeter scale. Translating these concepts to larger scales for practical purposes is an obvious next step; however, the size, weight, and method of actuation present a new set of problems to overcome. We have developed large-scale folding polyhedra to rapidly and noninvasively enclose marine organisms in the water column. The design is based on an axisymmetric dodecahedron net that is folded by an external assembly linkage. Requiring only a single rotary actuator to fold, the device is suited for remote operation onboard underwater vehicles and has been field-tested to encapsulate a variety of delicate deep-sea organisms. Our work validates the use of self-folding polyhedra for marine biological applications that require minimal actuation to achieve complex motion. The device was tested to 700 m, but the system was designed to withstand full ocean depth (11 km) pressures. We envision broader terrestrial applications of rotary-actuated folding polyhedra, ranging from large-scale deployable habitats and satellite solar arrays to small-scale functional origami microelectromechanical systems.

INTRODUCTION

The oceanic water column is the largest and least explored environment on Earth, and we are only beginning to understand the diversity, distribution, and spatiotemporal variability of deep-sea midwater biology (*1*, *2*). It is estimated that up to a million species remain undescribed in the deep pelagic zone (*3*, *4*). Although there is an array of technologies (*5*) available to marine biologists once a submarine or remotely operated underwater vehicle (ROV) reaches the benthic environment, the pelagic environment is much less explored and studied because of the difficulty of interacting with marine life in open water. Challenging this endeavor is the fact that many pelagic animals are often gelatinous or delicate and require extreme care in their collection and preservation. Deep-sea net tows offered the first window into pelagic biology, beginning with a modified version of the Agassiz trawl in the 1920s (named after Harvard biologist Alexander Agassiz) and followed by a wide array of innovative trawls that continue to this day (*6*, *7*). These are effective at enclosing more robust animals (e.g., fish and crustaceans), but gelatinous organisms (e.g., jellyfish, ctenophores, and siphonophores) are mostly destroyed or shredded in towed nets. To address this, many tools and techniques that focus on improving discrete midwater sampling from deep-sea vehicles have been developed. These fall into two categories, each with their own advantages and trade-offs: The detritus sampler (D sampler) is a cylinder with two lids that open and close in tandem (Fig. 1C), requiring fine control of the entire subsea platform to position it (Fig. 1A), and the suction sampler type consists of an inlet tube, suction pump, and storage bucket that can destroy very delicate specimens when they travel through the plumbing (Fig. 1B). Modifications and improvements on both methods have been introduced (*8*), but the fundamental approach has remained the same, offering limited options to midwater scientists attempting to rapidly capture delicate organisms with minimal disturbance to their tissues.

Origami, the Japanese art of paper folding, has recently come to the forefront of robotics research as a viable strategy to create three-dimensional (3D) structures from 2D layers (*9*–*18*). Drawing inspiration from this approach, we present a unique device for midwater interaction using rotary-actuated folding polyhedrons. With a single-axis rotational input, a mechanical linkage system transforms the net of a polyhedron with n degrees of freedom (DOFs) into a 1-DOF layer. Our folding polyhedrons quickly encapsulated delicate specimens for imagery, collection, and in situ experimentation purposes. Our most effective design was the RAD (rotary actuated dodecahedron), a 3D-printed axisymmetric dodecahedron with an external assembly linkage that incorporates modular components, low-friction bearings, and flexible seams (Fig. 1C). Prototypes were first tested in aquaria and then field-tested on an ROV to successfully capture delicate organisms in the deep sea.

This work formed the basis for a scale-independent strategy to construct 3D objects from 2D layers using a single rotary actuator. This approach has three advantages: (i) Only one actuator is needed, (ii) no sensing is required because fold angles are mechanically programmed, and (iii) building in 2D layers has the potential to leverage well-developed, high-throughput, parallel assembly planar manufacturing techniques such as photolithography, printed circuit microelectromechanical systems (PC-MEMS) (*19*, *20*), and lamination. Although midwater sampling offered a practical demonstration of our technology on a large scale, we envision broader applications including manufacturing of 3D devices from 2D layers, encapsulating 3D scanners for reality capture systems (*21*), self-deployable habitats, foldable solar arrays for satellites, deployable mirrors for space telescopes, and medical devices.

RESULTS

Rotary-actuated dodecahedrons

The dodecahedron was chosen to demonstrate rotary-actuated folding polyhedrons because it shows (i) the transformation of a 10-DOF system to a 1-DOF system, (ii) simultaneous folding of more than two

[1]School of Engineering and Applied Sciences, Harvard University, Cambridge, MA 02138, USA. [2]Wyss Institute for Biologically Inspired Engineering, Boston, MA 02115, USA. [3]Department of Ocean Engineering, University of Rhode Island, Narragansett, RI 02881, USA. [4]Graduate School of Design, Harvard University, Cambridge, MA 02138, USA. [5]Baruch College and The Graduate Center, PhD Program in Biology, City University of New York, New York, NY 10010, USA. [6]Radcliffe Institute for Advanced Study, Harvard University, Cambridge, MA 02138, USA.
*Corresponding author. Email: zhierntheoh@gmail.com

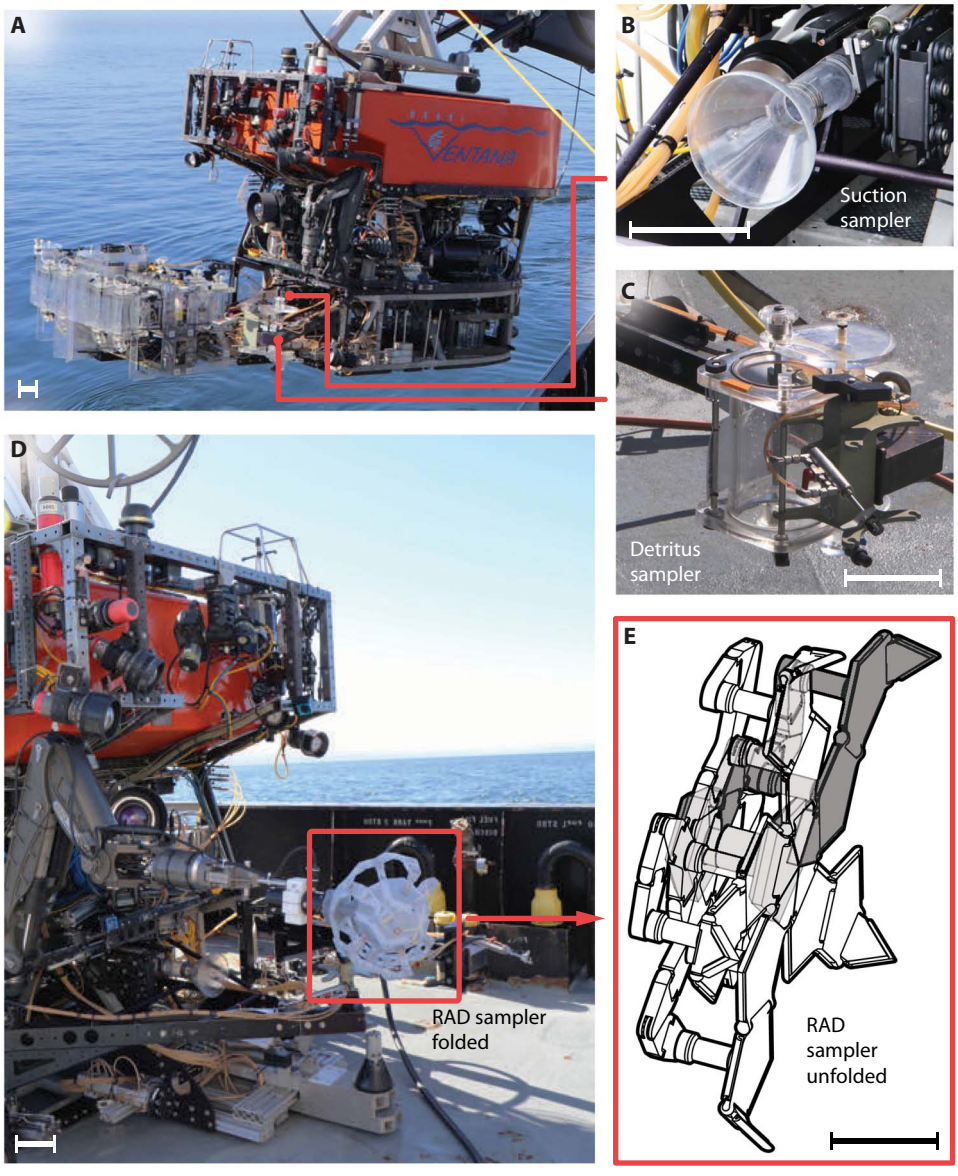

Fig. 1. State-of-the-art midwater sampling tools. (**A**) ROV *Ventana* outfitted with a rack of D samplers and a suction sampler; the ROV thrusters are used to maneuver D samplers into position. (**B** and **C**) Close-up views of the suction sampler and D sampler. (**D**) RAD sampler mounted on the ROV *Ventana* via a robotic arm. (**E**) Magnified schematic view of the RAD sampler in its unfolded configuration. Scale bars, 0.1 m.

panels along each folding arm, and (iii) coordination of 3D folds with only one rotary actuator. In an ideal scenario with no gravity and joints with no backlash, attaching a rotary actuator to any face can fold the net into its 3D shape. However, the presence of gravity, mass of the linkages, friction, and backlash led to arranging the net in an axisymmetric manner to distribute the load evenly about the central assembly and folding links (Fig. 2A).

To create line symmetric nets, we split the closure panel of the dodecahedron into five triangular segments. All panels were planar except for the last panel on each arm, which had triangular tips angled upward to enable closure of the dodecahedron. The resulting net is not a regular net but a pseudo general net (*22*). Our general net design allowed for cutting the polyhedron along lines interior to its face, allowing axisymmetry (Fig. 2B).

To reduce the effects of friction, we used lightweight fluoropolymer bearings (Rulon). Rotational joints were 3D-printed to minimize weight by reducing the number of fasteners and bearings, leading to a reduction in torque required for folding at the cost of backlash. To quantify the effect of backlash on the kinematics of the fold and to test the 3D-printed folding unit against the kinematic model (a detailed derivation of the model is presented in eqs. S1 to S15), we placed a single folding unit of the RAD sampler in a motion capture arena to track the output folding angle θ_1 as the input rotation angle θ_6 varied (angles defined in Fig. 5B). The resulting measurement showed a high correlation with the kinematic model over 34 motion trials (fig. S3).

Soft edges were added to the scaled-up device as a design element to offer a degree of compliance during the closing sequence. The soft edges, shown in Fig. 3, were silicone gaskets that covered hard edges that might otherwise come in contact with target samples, mitigated the effects of backlash and misalignments in the joints, and added robustness to the structure by building a passive mechanical buffer against overdriving the mechanism at the end of its fold sequence (Fig. 2C). The cross-sectional shape of the soft edges (Fig. 3B) was designed to be glued over the corner of the dodecahedron panels, with a curved cantilever beam protruding outward. The cantilevered shape ensured that the force of gasket deformation was relatively low unless the cantilever was fully compressed against the side of the panel. The cantilever portion of the gasket was deflected by at least 2 mm when the sampler was in its fully closed position, creating a light seal. The soft edges allowed the system to be driven below or beyond the intended closure point without compromising the seal or risking damage to the structure, whether due to misalignment, backlash in the joints, or operator error.

In the current prototype system, the motion of the sampler was entirely controlled by the operator with the use of a joystick that interfaced with the ROV control panel on the boat. This allowed the ROV pilot or another operator to control the closure of the RAD sampler. Any motion of the sampler stopped when pressure was released on the joystick. This meant that the operator visually determined whether a target specimen was clear of pinching before fully closing the arms of the sampler and could fully reverse the closure at any time if there was cause for concern. The operator must also release the joystick to prevent overdriving the arm linkages in the process of fully closing or opening the RAD sampler. The rate of closure was controlled by the joystick, and the maximum

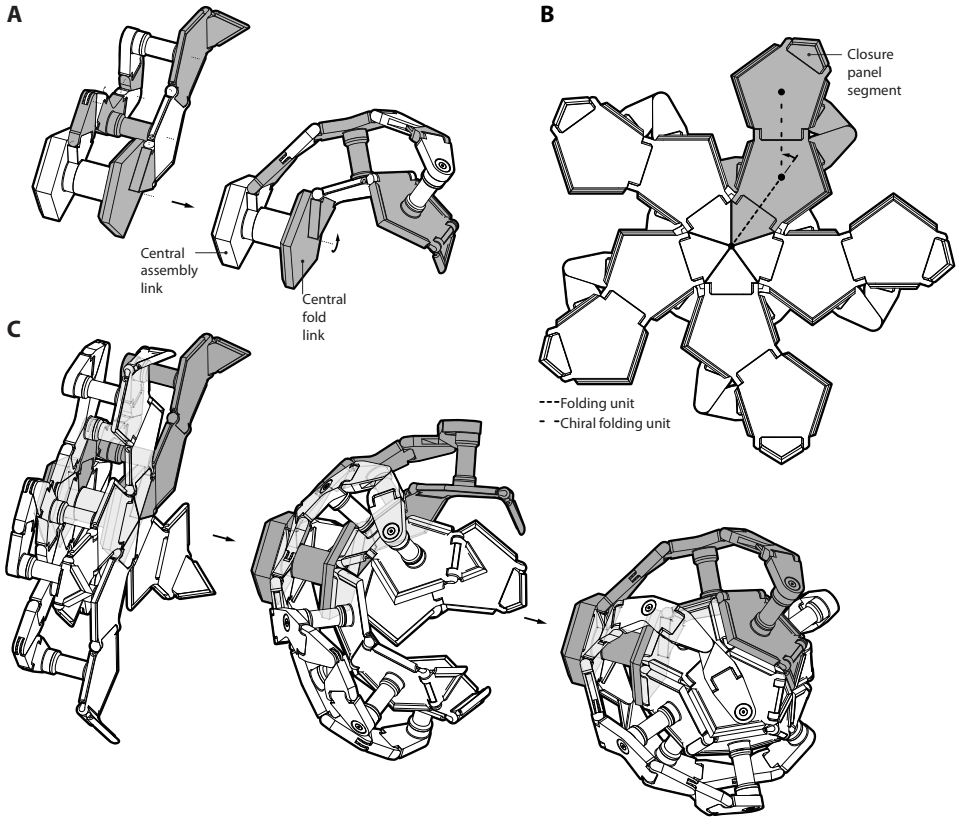

Fig. 2. RAD sampler design. (**A**) One arm of the RAD sampler with revolute joints shown as dotted lines. A fold is initiated by rotating the central fold link with respect to the central assembly link. (**B**) Axisymmetric dodecahedron net. Each arm is made by connecting a folding unit with its rotated chiral counterpart. (**C**) Folding sequence when encapsulating a marine organism.

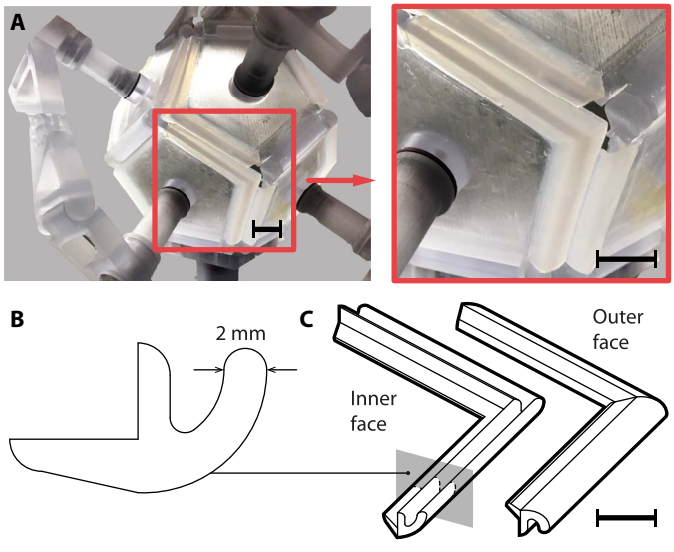

Fig. 3. Details of seal design. (**A**) RAD sampler (left), with close-up view (right) indicating the soft edges that form the light seal. (**B**) Cross-sectional shape of the gasket with curved cantilever design used to minimize deflection forces and accommodate alignment variance. (**C**) Inner and outer faces of one of three gasket shapes made (with the same cross section) to cover the RAD sampler panel edges. Scale bars, 15 mm.

achievable velocity at full deflection of the joystick can be limited with software adjustments. The soft gaskets around the edges of the sampler enabled the sampler to be effectively closed when underdriven by several millimeters and prevented damage when the sampler was driven several millimeters beyond the intended angle of closure.

Scaling and field demonstrations

Deep-sea midwater organisms vary widely in size and shape, making it impossible to design a collection device that is suited for every deep-sea interaction opportunity. However, most suction samplers and D samplers have a sampling volume of 3 to 10 liters, making them suitable for capturing small- to medium-sized specimens. In this instance of a folding dodecahedron, the design of the encapsulated volume dictated an unfolded diameter that was substantially larger than that of the device in its folded state. Because all deep-sea vehicles have limited space available for sampling and imaging, this required a compromise between sampling volume and practicality. Furthermore, prototyping through 3D printing was subject to size limits of the printer's print volume, making the RAD design size a subjective balance between practical usage, modularity, and print volume. For these reasons, the final design had an unfolded diameter of 0.518 m and a folded diameter of 0.207 m. The RAD had an encapsulated volume of 3.11×10^{-3} m^3 (about 3 liters), which is within the same range of existing midwater samplers (*23*).

Owing to the 3D-printed polymer specific gravity of 1.15, the mass of the 3D-printed assembly was largely supported by buoyancy forces, resulting in faster actuation when submerged in water relative to actuation in air (see hydrodynamic and buoyancy force estimation in the Supplementary Materials). We attached the RAD to a short boom and successfully collected and released moon jellyfish (*Aurelia aurita*) in a large aquarium (Mystic Aquarium, Mystic, CT). After these tests, design iterations shifted toward modularity to make the device robust and repairable for deployment in the deep sea.

The main differences between water in laboratory conditions and in the deep sea are ambient pressure and density (which are dependent on temperature, salinity, and pressure). The sampler was designed to have no internally sealed voids to reduce the risk of implosion due to the increase in hydrostatic pressure as the sampler descended with the ROV. Furthermore, the sampler was also made of incompressible materials. Therefore, the ambient pressure did not affect its operation. As the depth increased, the temperature of the water decreased, whereas the salinity increased, resulting in an increase of viscosity by about 50% (*24*). However, although the viscosity has increased, the resulting change in the Reynolds number is unlikely to affect the drag coefficient (*25*). Estimates for seawater density suggest that seawater density at 650 m is 0.4% higher than that in laboratory conditions. Collectively, these data indicate that hydrodynamic drag and buoyancy forces were

similar in both laboratory conditions and the deep sea (see force estimate spreadsheet in the Supplementary Materials). Therefore, the dynamic performance of the RAD sampler was expected to behave similarly in both laboratory and deep-sea conditions.

The ocean is notoriously harsh on scientific equipment. Therefore, to design a practical RAD enclosure device, close consultation with experienced ROV engineers and pilots at the Monterey Bay Aquarium Research Institute (MBARI) was crucial to the design process. Ultimately, the RAD was used as a tool mounted on the ROV's manipulator arm (Fig. 1D). The motor providing the rotary input to the RAD was proportionally controlled from the surface using a simple joystick interface. The RAD was positioned by using both the manipulator arm and the ROV's thrusters. Collections of highly mobile organisms, such as squid and fragile-tissue jellyfish, were encapsulated rapidly before they could escape, at depths ranging from 500 to 700 m (Fig. 4, A to L). The rotary actuator chosen for the RAD sampler was an oil-filled pressure-compensated unit with an ocean depth rating of 11 km, and hence, the system's depth range was only limited by the platform on which it was operated.

DISCUSSION

The use of self-folding polyhedra to create 3D objects from 2D sheets has its roots in electric circuit design and molecular chemistry (*26*–*28*), with a broad range of applications envisioned for the future (*29*). However, in practice, few designs exist beyond miniature and paper models, and practical demonstrations are a rarity. The challenge of encapsulating delicate organisms in the water column is a known limitation to deep-sea science and presents a unique opportunity to validate the concept of large-scale folding polyhedra in the field. Progress in large-scale fabrication of such complex designs is further aided by recent advances in photopolymer 3D printing, which directly contributed to the success of this work.

Folding polyhedron theory

3D objects can be approximated by polyhedra. Whether every convex polyhedron has a net remains an open problem (*30*, *31*), but Platonic and Archimedean solids are readily unfolded into their nets. To fold a polyhedron from its net, one can manually fold it (*32*) or use a range of self-folding techniques, such as embedding shape memory composites along fold creases (*33*), using surface tension to drive folding (*34*), and

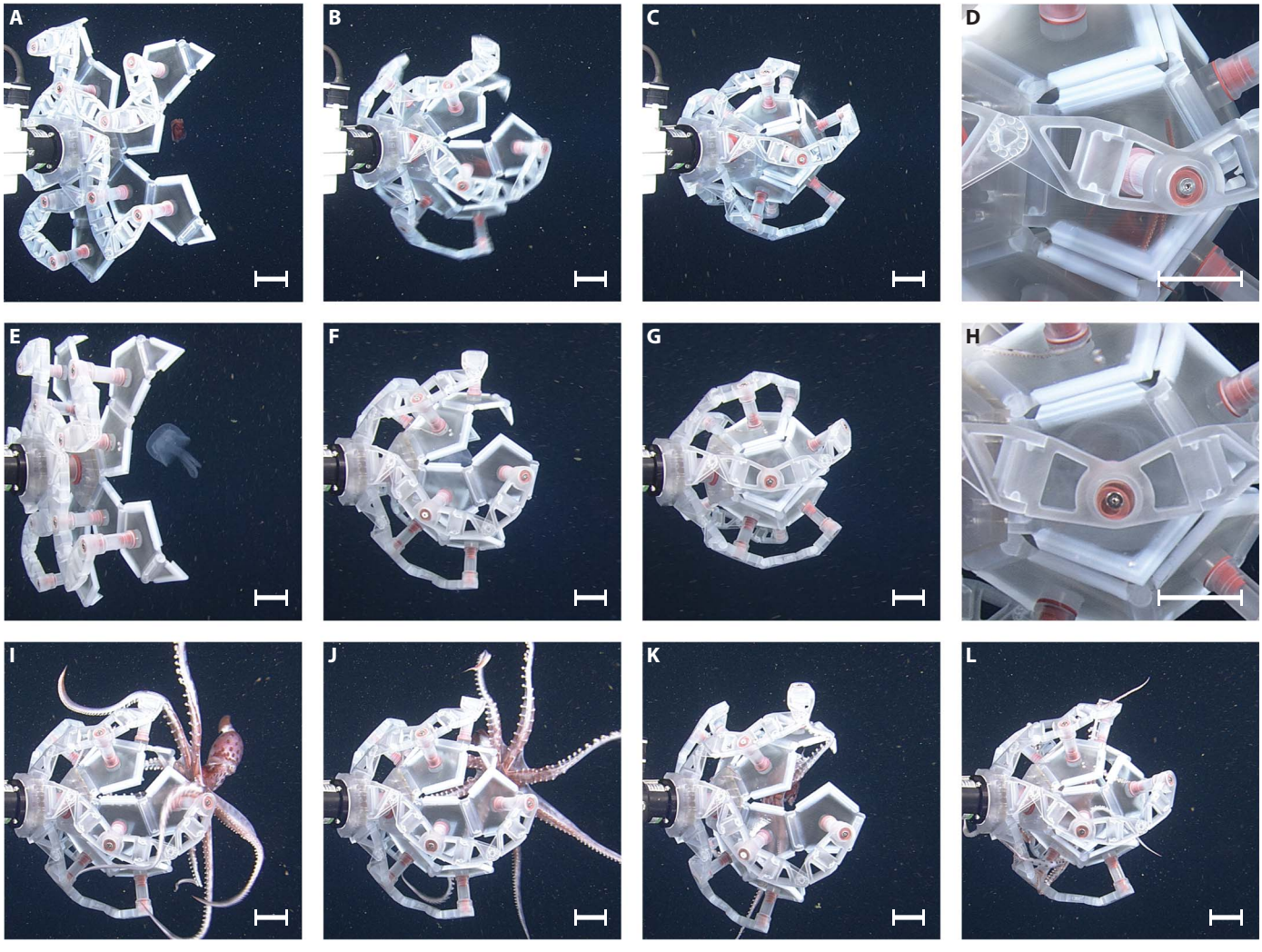

Fig. 4. Capture sequences of a RAD-equipped deep-sea vehicle operating in the Monterey Bay Canyon. (**A** to **D**) The RAD enclosing an *Oegopsina* sp. deep-sea squid at 563-m depth. (**E** to **H**) RAD sampler encompassing the scyphomedusa *Stellamedusa ventana* at 644 m. (**I** to **L**) RAD interacting with a *Stigmatoteuthis* sp. deep-sea squid at 645-m depth (video of various collections is provided in the Supplementary Materials). Scale bars, 0.05 m.

folding through the release of stress in prestrained laminates (*35*). Instead of using actuators to fold every link pair and relying on mechanical joint stops to passively control fold angles, we present a method to transform an *n*-DOF net into a 1-DOF net. Fold angles were mechanically programmed, and folding was driven by a single rotary actuator. This method has four benefits: (i) a reduction in the number of actuators and sensors, (ii) no computation is needed for assembly, (iii) a reduction in system integration complexity, and (iv) the structure can be reversibly folded and unfolded. The plane symmetric Bricard linkage (*36*) is the fundamental folding unit for constructing 1-DOF foldable Platonic polyhedra (Fig. 5). We considered its simplest form where $a_{61} = a_{12} = a$, $a_{23} = a_{34} = a_{45} = a_{56} = b$, $R_3 = R_5 = 0$, and $R_2 = R_6 = r$. The folding unit has three key design parameters: (i) a, the characteristic dimension of the folding unit; (ii) θ_s, the initial offset angle between link 5 and link 6 when the folding unit is in its flat unfolded configuration; and (iii) r, the link offset distance between the assembly layer and the folding layer (Fig. 5A). Together, they form two nondimensional variables $\hat{r}$ and $\hat{b}$, where $\hat{r} = \frac{r}{a}$ represents the normalized distance between the assembly linkage layer and the folding linkage layer and $\hat{b} = \frac{b}{a} = \frac{1}{2\cos\theta_s}$ represents the normalized length of the assembly links.

For folding to occur in both directions, θ_s has to be greater than zero (Fig. 6). However, as the symmetry of bidirectional folding increases, mechanical advantage decreases during fold initiation (when the fold angle θ_1 is zero). On the other hand, increasing $\hat{r}$ improves mechanical advantage by lengthening the moment arm of the folding torque. This improvement in mechanical advantage is offset by the decrease in how far θ_1 can rotate (a detailed derivation of the kinematics and mechanical advantage is found in eqs. S1 to S19). Knowing the kinematic and mechanical advantage trade-offs enables the designer to choose the folding unit parameters required to fold a desired 3D shape and size an appropriate actuator for folding of the net.

At first glance, a rotary actuator along the rotation axis connecting link 6 and link 1 would suffice to initiate a fold. However, the goal is to simultaneously fold all the polygonal faces of a convex polyhedron by using only one rotary actuator. By connecting each folding unit with its chiral through joining link 2 with link 5′ and link 1 with link 6′, the

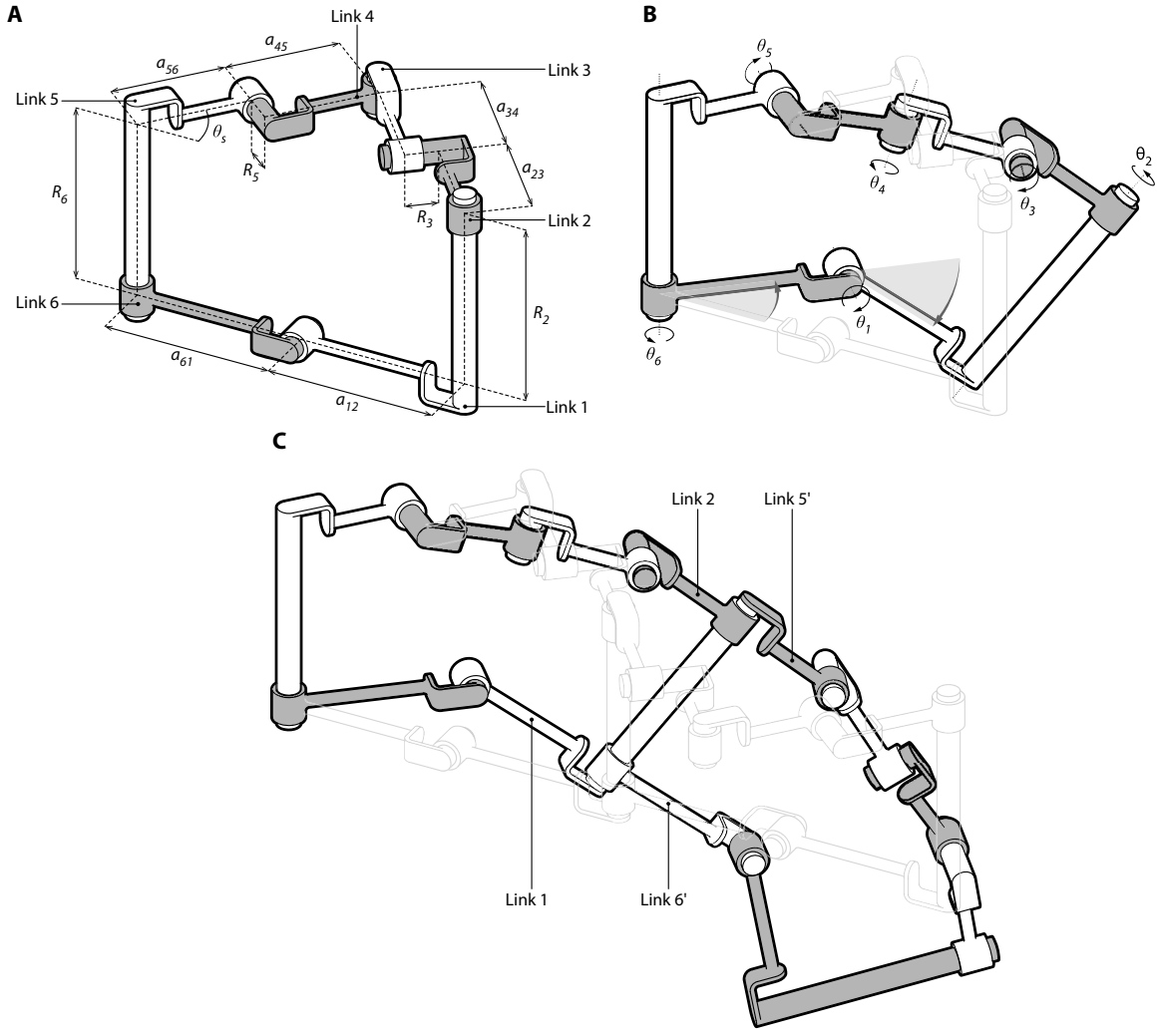

Fig. 5. Folding unit based on the plane symmetric Bricard linkage. (**A**) Six links are connected to each other by revolute joints. The linkage is separated into two layers: a folding linkage layer and an assembly linkage layer. The folding linkage layer consists of link 1 and link 6. The assembly linkage layer is on top of the folding linkage layer and comprises the remaining four links. (**B**) As link 6 rotates about link 5, the assembly layer folds link 1 with respect to link 6. (**C**) By joining a folding unit with its chiral (prime symbol denotes links of the chiral folding unit) by connecting link 1 to link 6′ and link 2 to link 5′, rotation of link 1 about link 6 propagates down the chain.

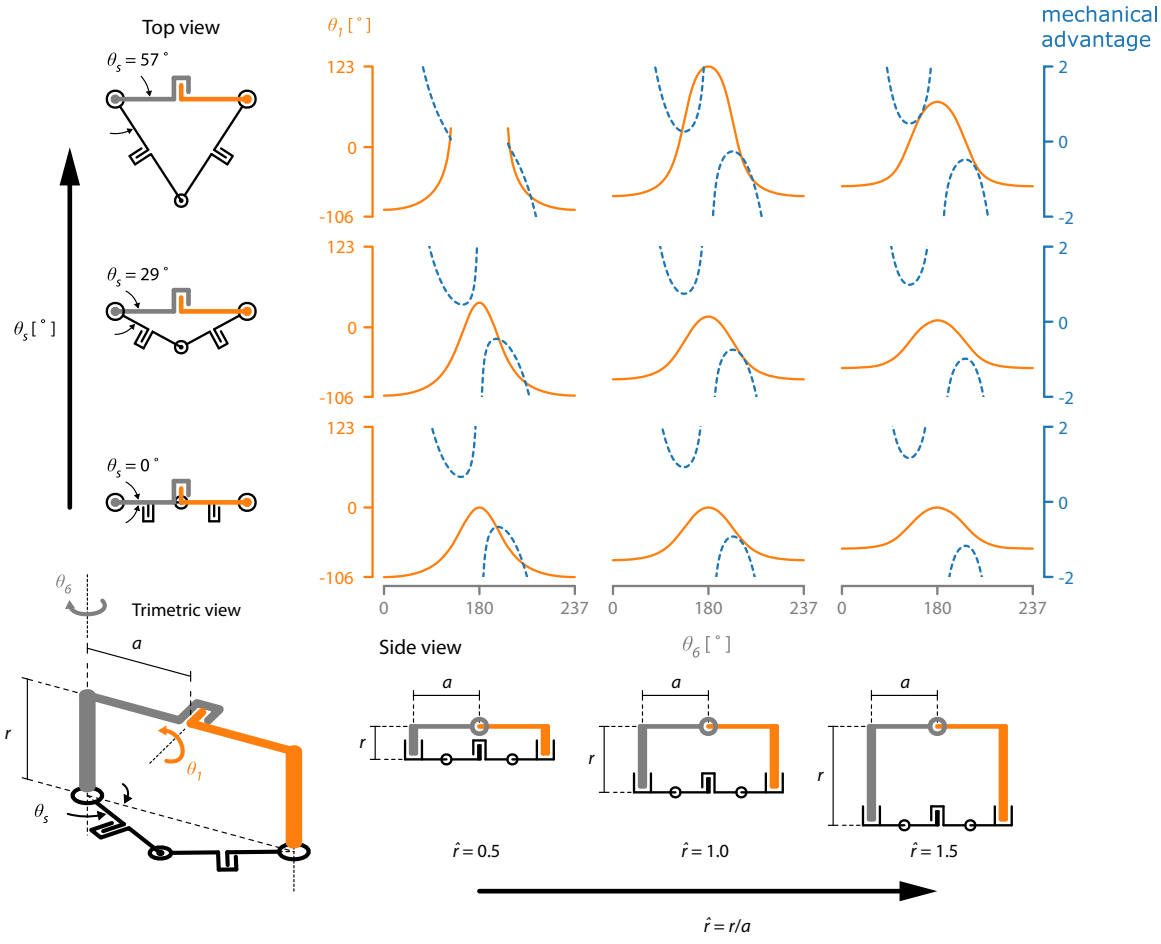

Fig. 6. Kinematic and mechanical advantage trade-off study. As initial offset angle (θ_s) of the folding unit increased, bidirectional folding became more symmetric. When normalized distance between the assembly linkage layer and the folding linkage layer ($\hat{r}$) increased, the corresponding minimum mechanical advantage increased.

rotation of link 6 about link 5 propagates down the chain (Fig. 5C). By replacing link 6 and link 1 with an equilateral triangle, square, or pentagonal polygonal panel, where the folding axes lie on the edges of each panel, the folding unit becomes the building block for creating all five Platonic polyhedra (tetrahedron, cube, octahedron, dodecahedron, and icosahedron).

The RAD sampler, built using folding polyhedron theory, represents a technological advance for sampling large midwater specimens. The ability to rapidly encapsulate delicate organisms in a 3D environment using a simple mechanical interface is particularly desirable for remote exploration systems. 3D reconstruction imaging (*37*) and velocimetry measurements (*38*) of in situ specimens may benefit from a sensorized RAD, making it an efficient deployable mechanism for observing zooplankton while causing minimal disturbance to the specimen. Similarly, studies on physiology may be possible by using the RAD as an in situ biological chamber. Once the organism is temporarily enclosed in the chamber, additional methods could be developed to obtain DNA and RNA from the target organism as well as environmental DNA from the surrounding water. This opens the possibility to obtain 3D imagery, physiological measurements, and potentially the genome and transcriptome of a deep-sea delicate pelagic organism and then to release it unharmed. Because of the simplicity of the rotary-actuated design, the RAD is suitable for use on autonomous platforms that have both weight and power restrictions.

In future generations of the prototype, the RAD may be adapted to incorporate visual and force feedback mechanisms. This will enable the RAD sampler to interact with delicate deep-sea specimens, such as benthic siphonophores and some mobile faunas. Visual feedback could come from cameras installed on the internal walls of the sampler, and force feedback could come from tactile sensors built into the soft gaskets around the edges. We are not aware of tactile sensors that have been demonstrated on deep-sea ROV systems but could further develop soft sensors similar to those presented by (*39*) and (*40*). Testing and operation of new sensors are challenging because they must resist shorting and corrosion due to the seawater salinity, withstand and operate in depths of up to 6000 m (about 60 MPa of hydrostatic pressure), and integrate with the existing ROV systems used for field testing.

By tailoring a folding polyhedron to assemble axisymmetrically using a single rotary actuator, we have created a design framework that is scalable and simple to operate. In the future, we imagine integrating folding polyhedrons with cameras for 3D imaging of the encased life forms, next-generation sequencing technology (*41*), or physiological measurement sensors for incubation studies to investigate how variables such as pH affect marine organisms (*42*). We anticipate a range of applications beyond interacting with pelagic biological organisms in the ocean. For example, the diameter of large aperture mirrors for space telescopes is limited by the fairing size of launch rockets (*43*). The RAD sampler can unfold to two and a half times its folded

diameter, allowing a scaled-up design to use the internal volume of the rocket's payload to achieve a wider aperture. Similarly, deployable habitats for extraterrestrial colonization may benefit from using rotary-actuated folding polyhedra to create multiple enclosed spaces from stacks of 2D linkage panels. Robotic manipulators may also benefit from using folding polyhedra to achieve power grasping capabilities with only one actuator (*44*, *45*). At the mesoscale (devices with sub-millimeter to centimeter length scales), a manufacturing technique termed PC-MEMS was developed to fabricate complex linkage mechanisms and robots (*19*, *20*). This technique was able to integrate a wide variety of materials, including composites, metals, ceramics, and soft materials such as polyimide and silicone films. Medical applications that require small-scale deployability or 3D shape transformation, such as laparoscopic needle–based biopsies, deployable stents, and micro-grippers (*46*), could leverage PC-MEMS and the folding polyhedron theory developed and demonstrated here. A video of a mesoscale partial dodecahedron fabricated using PC-MEMS is provided in the Supplementary Materials.

MATERIALS AND METHODS

SOLIDWORKS 2015 was used to create solid models that were printed on a Stratasys Connex500 3D printer using RGD810, a clear rigid thermoplastic-like photopolymer (www.stratasys.com). Rotary actuation was achieved by using a Saab Seaeye P00625 tilt motor rated for operation at full ocean depth and was controlled by using a Pololu 1378 Simple High-Power Motor Controller (www.pololu.com) operated via RS-232 serial interface. Field testing took place on 27 June 2017 using the ROV *Ventana* (www.mbari.org) during dive #4046 in Monterey Canyon, California. The device was mounted on the ROV's manipulator arm by using a standard T-handle arrangement and was launched and recovered in the fully folded position.

The seals, or soft edges, of the sampler were made from a silicone rubber (Dragon Skin 20, Smooth-On). Three differently shaped gaskets were designed to fit the edges of the polyhedron panels: one spanning a single edge, one spanning two edges (shown in Fig. 5C), and one for the tip of each of the arms. This was done to maximize continuous coverage of edges while avoiding any hindrance of joint motion. The cross section of the gasket (shown in Fig. 5B) is the same for each of the shapes and was designed to have a large area of contact with the corner of the 3D-printed dodecahedron panels and a curved cantilever to minimize the forces over a large range of deflection. Each gasket was formed by molding the silicone rubber in two-part molds printed on an Objet500 3D printer, in Stratasys TangoBlue resin. Once fully cured, the gaskets were trimmed of excess material from the molding process and attached to the sampler with silicone glue (Sil-Poxy, Smooth-On).

SUPPLEMENTARY MATERIALS

robotics.sciencemag.org/cgi/content/full/3/20/eaat5276/DC1
Fig. S1. Modified Denavit-Hartenberg convention.
Fig. S2. Visual description of plane symmetric Bricard linkage Denavit-Hartenberg parameters in table S1.
Fig. S3. Comparison of measured folding angle θ_1 with theory.
Table S1. Modified Denavit-Hartenberg parameters of folding unit.
Table S2. RAD morphological parameters.
Movie S1. RAD sampler capture sequences.
Movie S2. Folding dodecahedron at the mesoscale.
Motion capture data: Dataset_Segmented_fold.mat
Code: compare_device_to_theory.py and calculate_qF1.py
Estimate of hydrodynamic drag and buoyancy forces: force_estimate.xlsx
Reference (*47*)

REFERENCES AND NOTES

1. R. Kunzig, Deep-sea biology: Living with the endless frontier. *Science* **302**, 991 (2003).
2. T. T. Sutton, Vertical ecology of the pelagic ocean: Classical patterns and new perspectives. *J. Fish Biol.* **83**, 1508–1527 (2013).
3. B. H. Robison, Deep pelagic biology. *J. Exp. Mar. Biol. Ecol.* **300**, 253–272 (2004).
4. T. J. Webb, E. V. Berghe, R. O'Dor, Biodiversity's big wet secret: The global distribution of marine biological records reveals chronic under-exploration of the deep pelagic ocean. *PLOS ONE* **5**, e10223 (2010).
5. F. Russell, A net for catching plankton near the bottom. *J. Mar. Biol. Assoc. U.K.* **15**, 105–108 (1928).
6. S. C. Martin, L. L. Whitcomb, Fully actuated model-based control with six-degree-of-freedom coupled dynamical plant models for underwater vehicles: Theory and experimental evaluation. *Int. J. Robot. Res.* **35**, 1164–1184 (2016).
7. P. Wiebe, M. Benfield, Zooplankton sampling with nets and trawls, in *Measurement Techniques, Sensors and Platforms* (Elsevier, 2009), pp. 70–86.
8. R. F. Tusting, R. C. Tietze, K. R. Reisenbichler, Special-purpose samplers at HBOI. *Oceanograph. Lit. Rev.* **9**, 1065 (1997).
9. M. Z. Miskin, K. J. Dorsey, B. Bircan, Y. Han, D. A. Muller, P. L. McEuen, I. Cohen, Graphene-based bimorphs for micron-sized, autonomous origami machines. *Proc. Natl. Acad. Sci. U.S.A.* **115**, 466–470 (2018).
10. S. J. P. Callens, A. A. Zadpoor, From flat sheets to curved geometries: Origami and kirigami approaches. *Mater. Today* **21**, 241–264 (2018).
11. S. Janbaz, N. Noordzij, D. S. Widyaratih, C. W. Hagen, L. E. Fratila-Apachitei, A. A. Zadpoor, Origami lattices with free-form surface ornaments. *Sci. Adv.* **3**, eaao1595 (2017).
12. S. Miyashita, S. Guitron, S. Li, D. Rus, Robotic metamorphosis by origami exoskeletons. *Sci. Robot.* **2**, eaao4369 (2017).
13. C. D. Onal, M. T. Tolley, R. J. Wood, D. Rus, Origami-inspired printed robots. *IEEE ASME Trans. Mechatron.* **20**, 2214–2221 (2015).
14. R. Gagler, A. Bugacov, B. E. Koel, P. M. Will, Voxels: Volume-enclosing microstructures. *J. Micromech. Microeng.* **18**, 055025 (2008).
15. B. Gimi, T. Leong, Z. Gu, M. Yang, D. Artemov, Z. M. Bhujwalla, D. H. Gracias, Self-assembled three dimensional radio frequency (RF) shielded containers for cell encapsulation. *Biomed. Microdevices* **7**, 341–345 (2005).
16. A. Legrain, J. W. Berenschot, N. R. Tas, L. Abelmann, Capillary origami of micro-machined micro-objects: Bi-layer conductive hinges. *Microelectron. Eng.* **140**, 60–66 (2015).
17. J. L. Silverberg, A. A. Evans, L. McLeod, R. C. Hayward, T. Hull, C. D. Santangelo, I. Cohen, Using origami design principles to fold reprogrammable mechanical metamaterials. *Science* **345**, 647–650 (2014).
18. A. Efimovskaya, Y.-W. Lin, A. M. Shkel, Origami-like 3-D folded MEMS approach for miniature inertial measurement unit. *J. Microelectromech. Syst.* **26**, 1030–1039 (2017).
19. P. S. Sreetharan, J. P. Whitney, M. D. Strauss, R. J. Wood, Monolithic fabrication of millimeter-scale machines. *J. Micromech. Microeng.* **22**, 055027 (2012).
20. D. M. Aukes, B. Goldberg, M. R. Cutkosky, R. J. Wood, An analytic framework for developing inherently-manufacturable pop-up laminate devices. *Smart Mater. Struct.* **23**, 094013 (2014).
21. H. Joo, T. Simon, X. Li, H. Liu, L. Tan, L. Gui, S. Banerjee, T. S. Godisart, B. Nabbe, I. Matthews, T. Kanade, S. Nobuhara, Y. A Sheikh, Panoptic studio: A massively multiview system for social interaction capture. *IEEE Trans. Pattern Anal. Mach. Intell.* (2017).
22. J. O'Rourke, *How to Fold It: The Mathematics of Linkages, Origami, and Polyhedra* (Cambridge Univ. Press, 2011).
23. N. A. Raineault, J. Flanders, A. Bowman, New frontiers in ocean exploration: The E/V *Nautilus*, NOAA ship *okeanos explorer*, and R/V *Falkor* 2017 field season. *Oceanography* **31**, 126 (2018).
24. M. H. Sharqawy, J. H. Lienhard, S. M. Zubair, Thermophysical properties of seawater: A review of existing correlations and data. *Desalin. Water Treat.* **16**, 354–380 (2010).
25. D. Lisoski, "Nominally 2-dimensional flow about a normal flat plate" (Technical Report, Graduate Aerospace Laboratories, California Institute of Technology, 1993).
26. P. J. Stang, B. Olenyuk, Self-assembly, symmetry, and molecular architecture: Coordination as the motif in the rational design of supramolecular metallacyclic polygons and polyhedra. *Acc. Chem. Res.* **30**, 502–518 (1997).
27. D. H. Gracias, J. Tien, T. L. Breen, C. Hsu, G. M. Whitesides, Forming electrical networks in three dimensions by self-assembly. *Science* **289**, 1170–1172 (2000).
28. D. H. Gracias, V. Kavthekar, J. C. Love, K. E. Paul, G. M. Whitesides, Fabrication of micrometer-scale, patterned polyhedra by self-assembly. *Adv. Mater.* **14**, 235–238 (2002).
29. G. M. Whitesides, B. Grzybowski, Self-assembly at all scales. *Science* **295**, 2418–2421 (2002).
30. E. D. Demaine, J. O'Rourke, *Geometric Folding Algorithms* (Cambridge Univ. Press, Cambridge, 2007).
31. A. Dürer, *The Painter's Manual: A Manual of Measurement of Lines, Areas, and Solids by Means of Compass and Ruler Assembled by Albrecht Dürer for the Use of All Lovers of Art with Appropriate Illustrations Arranged to be Printed in the Year MDXXV* (Abaris Books, 1977).

32. S. T. Brittain, O. J. A. Schueller, H. Wu, S. Whitesides, G. M. Whitesides, Microorigami: Fabrication of small, three-dimensional, metallic structures. *J. Phys. Chem. B* **105**, 347–350 (2001).
33. S. Felton, M. Tolley, E. Demaine, D. Rus, R. Wood, A method for building self-folding machines. *Science* **345**, 644–646 (2014).
34. T. G. Leong, P. A. Lester, T. L. Koh, E. K. Call, D. H. Gracias, Surface tension-driven self-folding polyhedra. *Langmuir* **23**, 8747–8751 (2007).
35. S. Xu, Z. Yan, K.-I. Jang, W. Huang, H. Fu, J. Kim, Z. Wei, M. Flavin, J. McCracken, R. Wang, A. Badea, Y. Liu, D. Xiao, G. Zhou, J. Lee, H. U. Chung, H. Cheng, W. Ren, A. Banks, X. Li, U. Paik, R. G. Nuzzo, Y. Huang, Y. Zhang, J. A. Rogers, Assembly of micro/nanomaterials into complex, three-dimensional architectures by compressive buckling. *Science* **347**, 154–159 (2015).
36. R. Bricard, Mémoire sur la théorie de l'octaèdre articulé. *J. Math. Pures Appl.* **3**, 113–148 (1897).
37. C. Briseño-Avena, P. L. D. Roberts, P. J. S. Franks, J. S. Jaffe, ZOOPS-O^2: A broadband echosounder with coordinated stereo optical imaging for observing plankton in situ. *Methods Oceanogr.* **12**, 36–54 (2015).
38. K. Katija, R. E. Sherlock, A. D. Sherman, B. H. Robison, New technology reveals the role of giant larvaceans in oceanic carbon cycling. *Sci. Adv.* **3**, e1602374 (2017).
39. H. Zhao, K. O'Brien, S. Li, R. F. Shepherd, Optoelectronically innervated soft prosthetic hand via stretchable optical waveguides. *Sci. Robot.* **1**, eaai7529 (2016).
40. R. K. Kramer, *Micro- and Nanotechnology Sensors, Systems, and Applications VII* (International Society for Optics and Photonics, 2015), vol. 9467, p. 946707.
41. D. R. Garalde, E. A. Snell, D. Jachimowicz, B. Sipos, J. H. Lloyd, M. Bruce, N. Pantic, T. Admassu, P. James, A. Warland, M. Jordan, J. Ciccone, S. Serra, J. Keenan, S. Martin, L. McNeill, E. J. Wallace, L. Jayasinghe, C. Wright, J. Blasco, S. Young, D. Brocklebank, S. Juul, J. Clarke, A. J. Heron, D. J. Turner, Highly parallel direct RNA sequencing on an array of nanopores. *Nat. Methods* **15**, 201–206 (2018).
42. M. Fine, D. Tchernov, Scleractinian coral species survive and recover from decalcification. *Science* **315**, 1811 (2007).
43. L. Puig, A. Barton, N. Rando, A review on large deployable structures for astrophysics missions. *Acta Astronaut.* **67**, 12–26 (2010).
44. A. Rodriguez, M. T. Mason, S. S. Srinivasa, Manipulation capabilities with simple hands, in *International Symposium on Experimental Robotics (ISER 2010)*, New Delhi and Agra, India, 18 to 21 December 2010.
45. H. Stuart, S. Wang, O. Khatib, M. R. Cutkosky, The ocean one hands: An adaptive design for robust marine manipulation. *Int. J. Robot. Res.* **36**, 150–166 (2017).
46. M. Johnson, Y. Chen, S. Hovet, S. Xu, B. Wood, H. Ren, J. Tokuda, Z. T. H. Tse, Fabricating biomedical origami: A state-of-the-art review. *Int. J. Comput. Assist. Radiol. Surg.* **12**, 2023–2032 (2017).
47. J. E. Baker, An analysis of the Bricard linkages. *Mech. Mach. Theory* **15**, 267–286 (1980).

Acknowledgments: We thank D. Vogt, C. Teeple, and A. Meckes for their technical assistance; the Motion Capture Laboratory at the Wyss Institute and J. Foster for their help with collecting kinematic data; the Mystic Aquarium and aquarists C. Sodergren, C. Gardiner, and T. DellaVentura for providing the assistance with aquarium testing; B. Robison, K. Reisenbichler, R. Sherlock, and the MBARI for the opportunity to work with the ROV *Ventana*; and C. Dawe, D. J. Osborn, M. Burczynski, and the crew of the R/V *Rachel Carson* for their assistance with field testing. **Funding:** This study was funded by the NSF Instrument Development for Biological Research (award #1556164 to R.J.W. and K. C. Galloway and #1556123 to D.F.G.), the NSF Graduate Research Fellowship (award #DGE1144152 to K.P.B.), and the National Academies Keck Futures Initiative of the National Academy of Sciences (award #NAKFI DBS21 to R.J.W. and D.F.G.). Any opinions, findings, conclusions, or recommendations expressed in this material are those of the authors and do not necessarily reflect the views of the NSF, the National Academies Keck Futures Initiative, or the National Academy of Sciences. We are grateful to the National Geographic Society Innovation Challenge (grant no. SP 12-14 to R.J.W. and D.F.G.) for inspiring this underwater soft robotic research. **Author contributions:** Z.E.T., B.T.P., and R.J.W. initiated the project. Z.E.T. designed, built, and analyzed the device. Z.E.T., B.T.P., K.P.B., G.W., J.C.W., and C.H. contributed to system design, development, and testing. Z.E.T., B.T.P., K.P.B., D.F.G., and R.J.W. wrote the paper. **Competing interests:** The authors declare that they have no competing interests. **Data and materials availability:** All data needed to evaluate the conclusions in the paper are present in the paper or the Supplementary Materials. Field research was conducted under California Department of Fish and Wildlife Permit #SC-2506 to MBARI.

Submitted 9 March 2018
Accepted 18 June 2018
Published 18 July 2018
10.1126/scirobotics.aat5276

Citation: Z. E. Teoh, B. T. Phillips, K. P. Becker, G. Whittredge, J. C. Weaver, C. Hoberman, D. F. Gruber, R. J. Wood, Rotary-actuated folding polyhedrons for midwater investigation of delicate marine organisms. *Sci. Robot.* **3**, eaat5276 (2018).

Science Robotics

Rotary-actuated folding polyhedrons for midwater investigation of delicate marine organisms

Zhi Ern Teoh, Brennan T. Phillips, Kaitlyn P. Becker, Griffin Whittredge, James C. Weaver, Chuck Hoberman, David F. Gruber, and Robert J. Wood

Sci. Robot. **3** (20), eaat5276. DOI: 10.1126/scirobotics.aat5276

Science Robotics (ISSN 2470-9476) is published by the American Association for the Advancement of Science. 1200 New York Avenue NW, Washington, DC 20005. The title *Science Robotics* is a registered trademark of AAAS.